

# State Normalization of Penetration Resistance and the Effect of Overburden Stress on Liquefaction Resistance

R. W. Boulanger<sup>1</sup>, I. M. Idriss<sup>1</sup>

<sup>1</sup>Department of Civil & Environmental Engineering, University of California, Davis, CA

**Abstract**—Standard procedures for estimating the liquefaction resistance of clean sand at different depths require correcting penetration resistances to an equivalent overburden stress of one atmosphere (i.e.,  $C_N$ ) and adjusting the cyclic resistance ratio for the effects of overburden stress (i.e.,  $K_\sigma$ ). These two factors have generally been developed empirically and independently of each other. These factors have recently been critically re-evaluated using a relative state parameter index ( $\xi_R$ ) as the basis for a consistent theoretical connection between them. In addition, the concept of state normalized penetration resistances has been introduced as an alternative method for representing the effect of overburden stress on cyclic resistance ratio. This paper expands upon these recent theoretical developments and presents relations that facilitate their implementation in engineering practice.

**Keywords**—Liquefaction, SPT, CPT, overburden stress

## INTRODUCTION

The cyclic resistance ratio (CRR) against triggering of liquefaction for sand at different depths is commonly estimated using [1]:

$$CRR = CRR_{\sigma=1, \alpha=0} K_\sigma K_\alpha \quad (1)$$

where  $CRR_{\sigma=1, \alpha=0}$  is the CRR for level ground conditions and an effective overburden stress ( $\sigma'_v$ ) of one atmosphere ( $P_a$ ),  $K_\sigma$  is the adjustment factor for the effects of  $\sigma'_v$  on CRR,  $K_\alpha$  is the adjustment factor for the effects of static shear stress on CRR,  $\alpha$  is the static horizontal shear stress ratio ( $\alpha = \tau_s / \sigma'_v$ ), and  $\tau_s$  is the static horizontal shear stress. The cyclic stress ratio (CSR) required to cause liquefaction is designated as CRR to distinguish it from the CSR induced by earthquake ground motions.  $CRR_{\sigma=1, \alpha=0}$  is commonly obtained through semi-empirical correlations to SPT or CPT penetration resistances that have been corrected to an equivalent  $\sigma'_v$  of 1  $P_a$  (1 atm  $\approx$  1 tsf  $\approx$  100 kPa) using the  $C_N$  factor as discussed later.

A critical reevaluation of the  $C_N$ ,  $K_\sigma$ , and  $K_\alpha$  factors was performed by [2] and [3] using existing experimental data and theoretical analyses, coupled with a relative state parameter index ( $\xi_R$ ) that provided a rational and practical means for establishing the inter-dependency of these three factors. In addition, the concept of state normalized penetration resistances was introduced as an alternative method for representing the effects of  $\sigma'_v$  on the CRR.

The resulting relations reduce the conservatism associated with the more common current relations that were developed independently of each other. Subsequently, relations for  $K_\alpha$  and  $K_\sigma$  as functions of SPT or CPT penetration resistances were derived by [4] and [5] to facilitate their implementation in practice. Similarly, this paper expands upon the theoretical developments in [2] and [3] by presenting equations for  $C_N$  and  $K_\sigma$  (or state normalization) that can be easily implemented in practice.

## RELATING CRR TO RELATIVE STATE PARAMETER INDEX

The relative state parameter index ( $\xi_R$ ) was derived by [2] based on the relative dilatancy index by [6].  $\xi_R$  is shown in Fig. 1 and is expressed as:

$$\xi_R = \frac{1}{Q - \ln \left( 100 \frac{(1 + 2K_o) \sigma'_{vo}}{3 P_a} \right)} - D_R \quad (2)$$

where  $Q$  is an empirical constant and  $K_o$  is the coefficient of lateral earth pressure at rest. The value of  $Q$  depends on grain type, with  $Q \approx 10$  for quartz and feldspar [6]. Reference [3] showed that the CRR could be expressed as a unique function of  $\xi_R$  based on the laboratory tests on reconstituted clean sand by [7] and [8] for a broad range of  $D_R$  and consolidation stresses.

Field CRR- $\xi_R$  relations were then derived from SPT- and CPT-based liquefaction correlations by correlating the penetration resistances to  $D_R$  (as discussed later) and then calculating  $\xi_R$  via equation (2). This derivation was performed because it is widely recognized that the CRR in the field can be significantly different from that measured on reconstituted specimens at the same  $D_R$  [9]. Revised SPT and CPT liquefaction correlations, as derived by [10] and [11], can be expressed as:

$$CRR_{\sigma=1, \alpha=0} = \exp \left\{ \frac{\left( \frac{(N_1)_{60}}{14.1} + \left( \frac{(N_1)_{60}}{126} \right)^2 \right)}{- \left( \frac{(N_1)_{60}}{23.6} \right)^3 + \left( \frac{(N_1)_{60}}{25.4} \right)^4} - 2.8 \right\} \quad (3)$$

$$CRR_{\sigma=1, \alpha=0} = \exp \left\{ \frac{\left( \frac{q_{cIN}}{540} + \left( \frac{q_{cIN}}{67} \right)^2 \right)}{- \left( \frac{q_{cIN}}{80} \right)^3 + \left( \frac{q_{cIN}}{114} \right)^4} - 3 \right\} \quad (4)$$

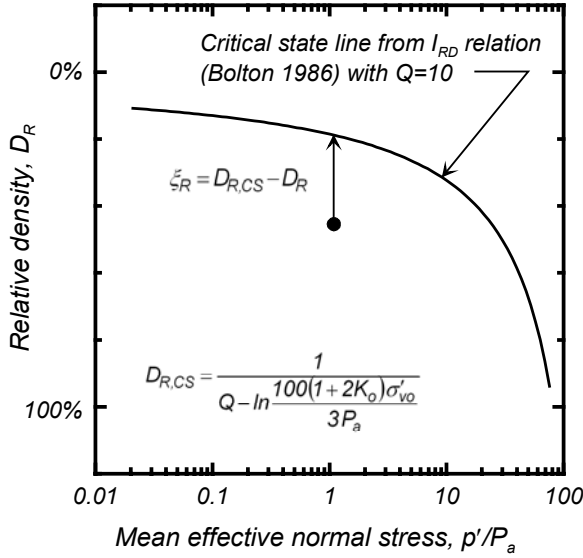


Fig. 1: Definition of the relative state parameter index.

where  $(N_1)_{60}$  is the SPT  $N$  value corrected to an equivalent energy ratio of 60% and overburden stress of one atmosphere, and  $q_{c1N}$  is the CTP tip resistance corrected to an equivalent overburden stress of one atmosphere and then divided by atmospheric pressure to eliminate units (i.e.,  $q_{c1N} = q_{c1}/P_a$ ). The corresponding field  $CRR-\xi_R$  relations are shown in Fig. 2; Note that the  $CRR-(N_1)_{60}$  and  $CRR-q_{c1N}$  relations in equations (3) and (4) were in fact adjusted to produce consistent  $CRR-\xi_R$  relations, as an improved basis for maintaining consistency between the two penetration-test based methods.

#### NORMALIZATION OF PENETRATION RESISTANCES

SPT and CPT penetration resistances depend on  $\sigma'_v$  and  $D_R$ , among other factors. Penetration resistances are thus normalized to an equivalent  $\sigma'_v$  of 1 atm to obtain quantities that uniquely relate to  $D_R$  for that sand (i.e., they no longer depend on  $\sigma'_v$ ),

$$(N_1)_{60} = C_N (N)_{60} \quad (5)$$

$$q_{c1} = C_N q_c \quad (6)$$

as illustrated in Fig. 3, and where  $C_N$  is the overburden normalization factor for penetration resistances. Reference [3] re-evaluated  $C_N$  relations based on theoretical and experimental data, and recommended the following for both SPT and CPT penetration resistances:

$$C_N = \left( \frac{P_a}{\sigma'_v} \right)^{0.784 - 0.521 D_R} \quad (7)$$

Reference [4] re-evaluated correlations between  $(N_1)_{60}$ ,  $q_{c1N}$  and  $D_R$  for the purpose of liquefaction evaluations,

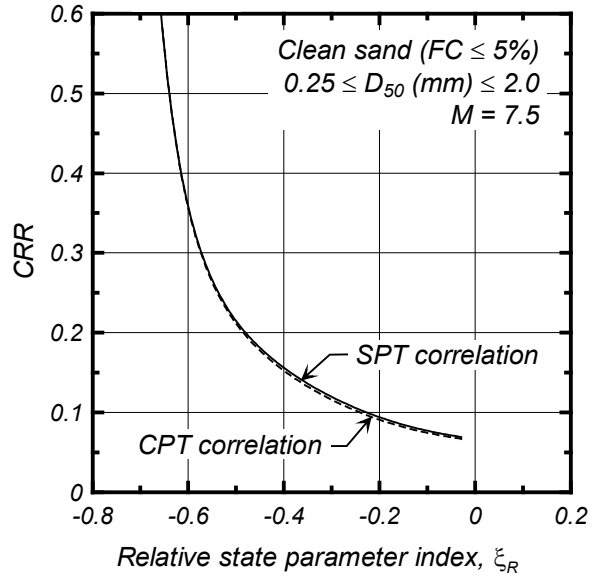


Fig. 2: Field  $CRR-\xi_R$  relations derived from recent liquefaction correlations for SPT [10] and CPT [11].

and recommended the following expressions:

$$D_R = \sqrt{\frac{(N_1)_{60}}{46}} \quad (8)$$

$$D_R = 0.478(q_{c1N})^{0.264} - 1.063 \quad (9)$$

for clean sands. This leads to the following expressions for determining  $C_N$  in practice,

$$C_N = \left( \frac{P_a}{\sigma'_vo} \right)^{0.784 - 0.0768 \sqrt{(N_1)_{60}}} \quad (10)$$

$$C_N = \left( \frac{P_a}{\sigma'_vo} \right)^{1.338 - 0.249(q_{c1N})^{0.264}} \quad (11)$$

with  $(N_1)_{60}$  limited to a maximum value of 46 and  $q_{c1N}$  limited to a maximum value of 254 in these  $C_N$  expressions, and with  $C_N$  limited to a maximum value of 1.7. The resulting  $C_N$  curves are plotted in Fig. 4 showing the increasing importance of  $D_R$  with increasing depth.

Solving for  $C_N$  requires iteration, but this is easily accomplished with most any software. For example, it can be accomplished in Excel by using a circular reference where the  $C_N$  cell depends on the  $(N_1)_{60}$  or  $q_{c1}$  cell, and then turning on the "Iteration" option under the Tools/Options/Calculation tab.

A uniform deposit of sand with the same  $D_R$  over all depths would therefore be expected to have the same  $(N_1)_{60}$  or  $q_{c1}$  values at all depths (Fig. 3). The sand in such a deposit would, however, become more contractive (i.e. increasing  $\xi_R$ ) with increasing depth (i.e., moving to the right in Fig. 1).

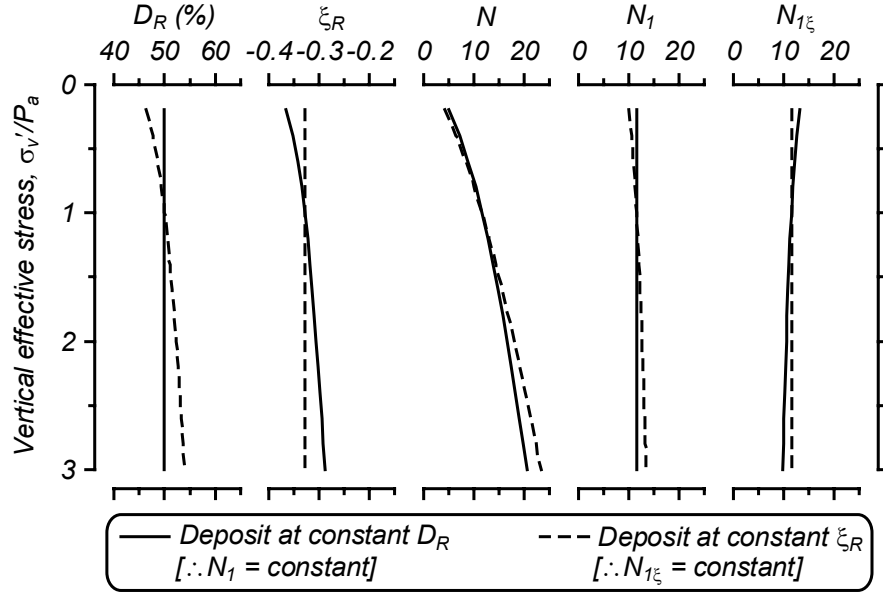


Fig. 3: Normalization of penetration resistance for overburden stress and relative state.

Reference [3] suggested that penetrations resistances could be further normalized to an equivalent  $\xi_R$  at  $\sigma'_v/P_a = 1$ , as:

$$N_{1\xi} = C_\xi C_N N \quad (12)$$

$$q_{c1\xi} = C_\xi C_N q_c \quad (13)$$

where  $C_\xi$  is the state normalization factor. As illustrated in Fig. 3, a uniform deposit of sand at the same  $D_R$  would therefore have  $(N_{1\xi})_{60}$  and  $q_{c1\xi}$  values that slowly decrease with depth, whereas a uniform deposit of sand at the same  $\xi_R$  over all depths would have  $D_R$  increasing with depth,  $(N_1)_{60}$  and  $q_{c1}$  values that increase slightly with depth, and  $(N_{1\xi})_{60}$  and  $q_{c1\xi}$  values that are constant with depth.

$C_\xi$  relations can be derived by first finding the difference in  $D_R$  that would give the same  $\xi_R$  at an equivalent  $\sigma'_v$  of 1 atm. This corresponds to the difference in the critical state  $D_R$  values ( $D_{R,CS}$  in Fig. 1) at the in-situ  $\sigma'_v$  and the reference  $\sigma'_v$  of 1 atm:

$$\Delta D_{R,CS} = \frac{1}{Q - \ln\left(100 \frac{1+2K_o}{3} \frac{\sigma'_v}{P_a}\right)} - \frac{1}{Q - \ln\left(100 \frac{1+2K_o}{3}\right)} \quad (14)$$

In most situations, the values for  $Q$  and  $K_o$  can reasonably be set at 10 and 0.45, in which case this expression can be simplified to:

$$\Delta D_{R,CS} = \frac{1}{5.85 - \ln\left(\frac{\sigma'_v}{P_a}\right)} - 0.171 \quad (15)$$

The  $C_\xi$  derivation can then be completed by determining how  $\Delta D_{R,CS}$  affects the  $(N_1)_{60}$  and  $q_{c1}$  values. For the SPT, the derivation uses equations (8) and (12) to get:

$$C_\xi = \left(\frac{D_R - \Delta D_{R,CS}}{D_R}\right)^2 \quad (16)$$

Combining equations (15) and (16) gives:

$$C_\xi = \frac{\left(\sqrt{(N_1)_{60}} - \frac{6.78}{5.85 - \ln\left(\frac{\sigma'_v}{P_a}\right)} + 1.16\right)^2}{(N_1)_{60}} \quad (17)$$

with  $(N_1)_{60}$  restricted to  $\leq 46$  in this expression. For the CPT, the relations are slightly different because of the different form of the relation between  $D_R$  and penetration resistance. The correspond  $C_\xi$  relations are:

$$C_\xi = \left(\frac{D_R - \Delta D_{R,CS} + 1.063}{D_R + 1.063}\right)^{3.788} \quad (18)$$

$$C_\xi = \frac{\left((q_{c1N})^{0.264} - \frac{2.09}{5.85 - \ln\left(\frac{\sigma'_v}{P_a}\right)} + 0.358\right)^{3.788}}{q_{c1N}} \quad (19)$$

with  $q_{c1N}$  restricted to  $\leq 254$  in this expression. The resulting  $C_\xi$  curves are plotted for the SPT in Fig. 5 and for the CPT in Fig. 6. Both sets of curves show  $C_\xi$  increasing with increasing  $D_R$  at  $\sigma'_v/P_a > 1$ , similar to how  $C_N$  increases with  $D_R$  at high  $\sigma'_v$ . The two sets of  $C_\xi$  curves are very similar at higher  $D_R$ , but have significant differences at low  $D_R$ . SPT  $C_\xi$  curves are also shown in

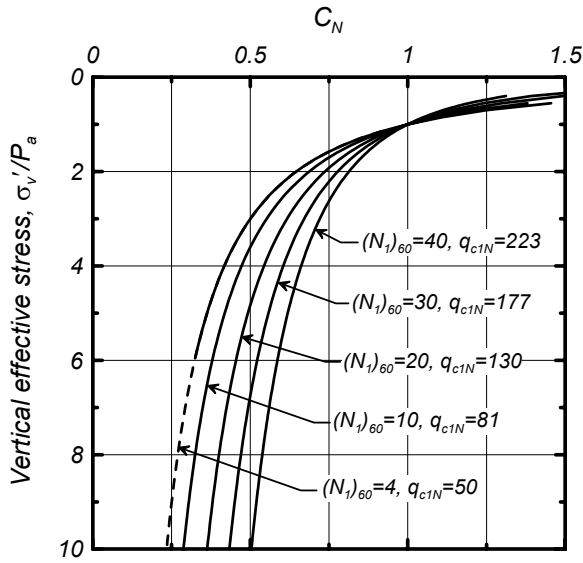


Fig. 4: Overburden normalization factor  $C_N$  by equations (10) or (11).

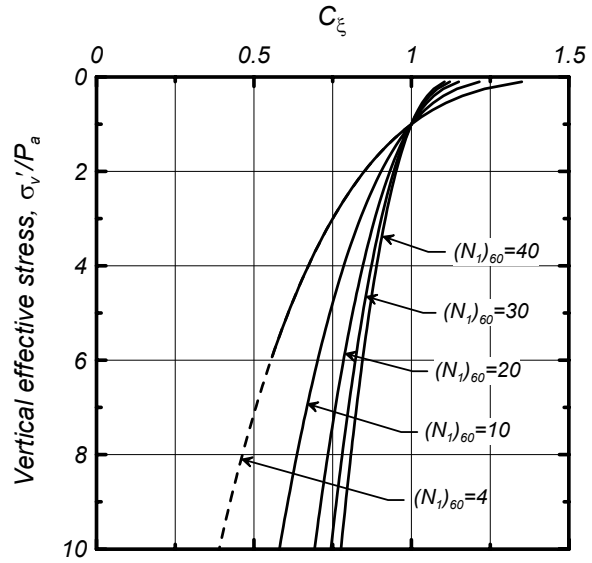


Fig. 5: State normalization factor  $C_{\xi}$  for range of  $(N_1)_{60}$  using equation (17).

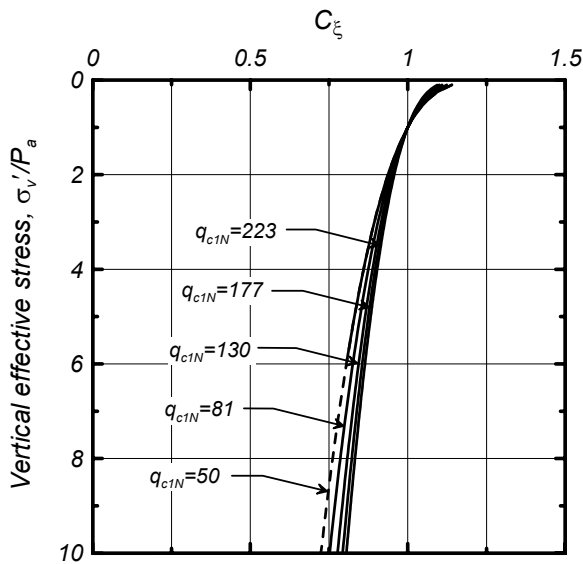


Fig. 6: State normalization factor  $C_{\xi}$  for range of  $q_{c1N}$  using equation (19).

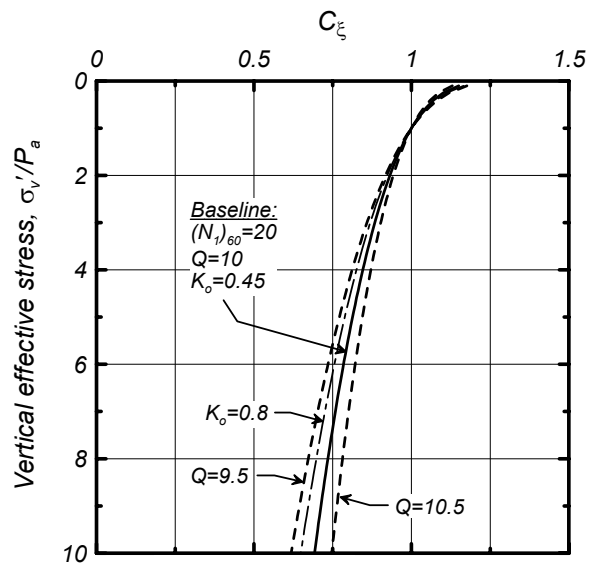


Fig. 7: Sensitivity of  $C_{\xi}$  to variations in  $K_o$  and  $Q$ .

Fig. 7 for reasonable variations in  $K_o$  and  $Q$  showing that the relations are reasonably stable for such variations in these input parameters. For liquefaction evaluations at  $\sigma'_v/P_a$  less than about 4, it can also be shown that it would be sufficient to have a single  $C_{\xi}$  relation that is independent of  $D_R$ , as:

$$C_{\xi} = \left( 1.23 - \frac{1.36}{5.85 - \ln\left(\frac{\sigma'_{vo}}{P_a}\right)} \right)^2 \quad (20)$$

The error involved in using this expression is minimal at  $\sigma'_v/P_a$  less than about 4, whereas it is recommended the full expressions given earlier be used at higher  $\sigma'_v$ .

#### ESTIMATING CRR FROM $(N_{1\xi})_{60}$ OR $q_{c1\xi}$

The cyclic resistance ratio (CRR) for clean sand can now be correlated directly to the state normalized penetration resistances. Since the field CRR- $\xi_R$  relation is unique (i.e., applies to any  $\sigma'_v$ ), and since  $\xi_R$  can be uniquely related to the  $(N_{1\xi})_{60}$  or  $q_{c1\xi}$  values, it follows that the corresponding CRR- $(N_{1\xi})_{60}$  and CRR- $q_{c1\xi}$

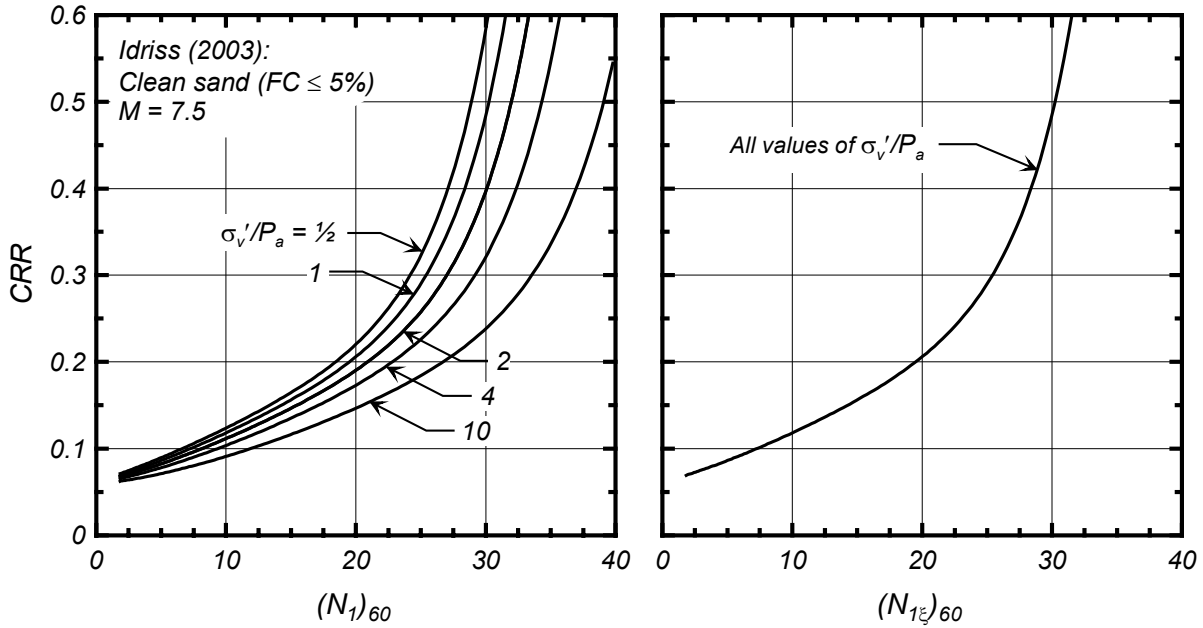


Fig. 8: CRR- $(N_1)_{60}$  relations for a range of effective overburden stresses and the unique CRR- $(N_{1\xi})_{60}$  relation.

relations are unique (i.e., they also apply to any  $\sigma'_v$ ). This is illustrated in Fig. 8 for the SPT relations, showing how the field CRR- $\xi_R$  relation in Fig. 2 results in CRR- $(N_1)_{60}$  relations that depend on  $\sigma'_v$  whereas a single CRR- $(N_{1\xi})_{60}$  relation applies to all  $\sigma'_v$ . Consequently, the CRR of clean sand can be evaluated using equations (3) and (4) rewritten as:

$$CRR = \exp \left\{ \frac{\left( \frac{(N_{1\xi})_{60}}{14.1} + \left( \frac{(N_{1\xi})_{60}}{126} \right)^2 \right)}{- \left( \frac{(N_{1\xi})_{60}}{23.6} \right)^3 + \left( \frac{(N_{1\xi})_{60}}{25.4} \right)^4} - 2.8 \right\} \quad (21)$$

$$CRR = \exp \left\{ \frac{\frac{q_{cl\xi N}}{540} + \left( \frac{q_{cl\xi N}}{67} \right)^2}{- \left( \frac{q_{cl\xi N}}{80} \right)^3 + \left( \frac{q_{cl\xi N}}{114} \right)^4} - 3 \right\} \quad (22)$$

Note that the shifting of the CRR- $(N_1)_{60}$  curves to the right as  $\sigma'_v$  increases in Fig. 8 is intuitively consistent with critical state soil mechanics concepts. In addition, equations (21) and (22) directly account for the effect of  $\sigma'_v$  on CRR through the state normalization of the penetration resistances, and hence an explicit  $K_\sigma$  factor is no longer needed.

#### EQUIVALENT $K_\sigma$ RELATIONS

The above approach can, however, also be used to derive equivalent  $K_\sigma$  factors that can be utilized within the

existing framework provided by equation (1) or just compared to  $K_\sigma$  relations that are currently in use. These equivalent  $K_\sigma$  relations can be derived as:

$$K_\sigma = \frac{CRR(\xi_R)}{CRR(\xi_{R1})} \quad (23)$$

where  $\xi_{R1}$  is the  $\xi_R$  that the sand would have if it was at the same  $D_R$  but with  $\sigma'_v = 1$  atm:

$$\xi_{R1} = \frac{1}{Q - \ln \left( 100 \frac{(1 + 2K_\sigma)}{3} \right)} - D_R \quad (24)$$

Alternatively, the equivalent result is obtained as:

$$K_\sigma = \frac{CRR \left[ (N_{1\xi})_{60} \right]}{CRR \left[ (N_1)_{60} \right]} \quad (25)$$

where  $CRR[(N_{1\xi})_{60}]$  and  $CRR[(N_1)_{60}]$  are obtained from equations (21) and (3), respectively. The same approach can be used for the CPT, which produces essentially the same  $K_\sigma$  relations as for the SPT because they have essentially identical CRR- $\xi_R$  relations (Fig. 2).

$K_\sigma$  curves derived from the field liquefaction correlations, using the above  $\xi_R$ -based framework can be reasonably approximated using the following relations:

$$K_\sigma = 1 - C_\sigma \ln \left( \frac{\sigma'_v}{P_a} \right) \quad (26)$$

$$C_\sigma = \frac{1}{18.9 - 17.3D_R} \leq 0.3 \quad (27)$$

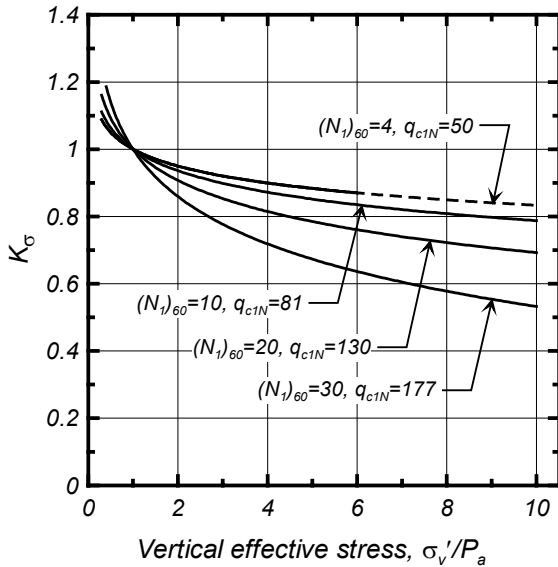


Fig. 9:  $K_\sigma$  relations derived from  $\xi_R$  relations.

which are based on  $Q \approx 10$ ,  $K_o \approx 0.45$ ,  $D_R \leq 0.9$ , and  $\sigma'_v/P_a \leq 10$ . The coefficient  $C_\sigma$  can be expressed in terms of  $(N_1)_{60}$  or  $q_{c1N}$  as follows:

$$C_\sigma = \frac{1}{18.9 - 2.55\sqrt{(N_1)_{60}}} \quad (28)$$

$$C_\sigma = \frac{1}{37.3 - 8.27(q_{c1N})^{0.264}} \quad (29)$$

with  $(N_1)_{60}$  and  $q_{c1N}$  limited to maximum values of 37 and 211, respectively, in these expressions. The resulting  $K_\sigma$  curves are shown in Fig. 9 for a range of  $(N_1)_{60}$  and  $q_{c1N}$  values. The derived  $K_\sigma$  curves are relatively insensitive to reasonable variations in the parameters  $Q$  and  $K_o$ , as shown in Fig. 10. Equations (27)-(29) closely approximate the  $K_\sigma$  relation by [12] when  $C_\sigma = 0.185$ , which corresponds to  $D_R = 0.78$ ,  $(N_1)_{60} = 28$  or  $q_{c1N} = 166$ . Equations (27)-(29) provide significantly higher  $K_\sigma$  values at high  $\sigma'_v$  compared to those recommended by [13] as shown in Fig. 11.

#### COMPARISON OF $K_\sigma$ VERSUS $C_\xi$ APPROACHES

It is noteworthy that  $K_\sigma$  curves derived using the  $\xi_R$  framework are dependent on the specific liquefaction correlation that is used [3]. For example, use of the SPT liquefaction correlation by [14] instead of the relation given in equation (26) produces  $K_\sigma$  curves that are somewhat different from those shown in Fig. 9. Furthermore, if the liquefaction correlation does not define CRR at higher penetration resistances (e.g., the CRR curve becomes vertical and is not defined for  $CRR > 0.6$ , such as in [14]), then the use of a  $K_\sigma$  relation cannot model the rightward shift of the CRR- $(N_1)_{60}$  relations with increasing  $\sigma'_v$  as shown in Fig. 8.

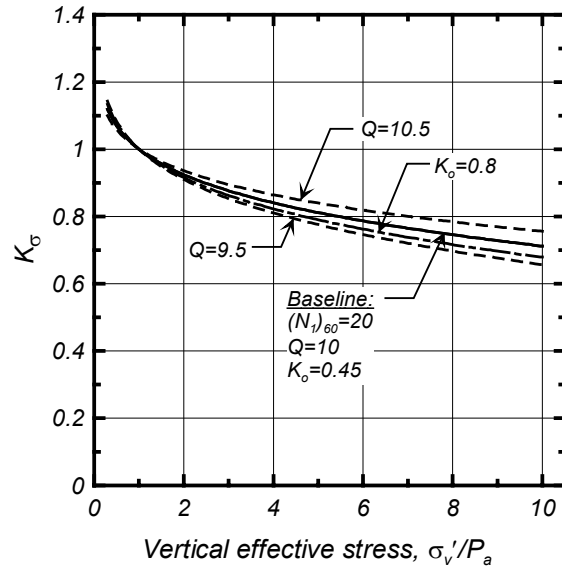


Fig. 10: Sensitivity of derived  $K_\sigma$  relations to  $K_o$  and  $Q$ .

Thus, the use of state normalized penetration resistances offers two main advantages over a traditional  $K_\sigma$  relation: (i)  $C_\xi$  factors are independent of the baseline liquefaction correlation, whereas  $K_\sigma$  relations strictly are not, and (ii)  $C_\xi$  factors properly capture the rightward shifting of the CRR- $(N_1)_{60}$  curves with increasing  $\sigma'_v$ , whereas a traditional  $K_\sigma$  relation may not.

#### EXAMPLE

The different approaches for incorporating high overburden stress effects in liquefaction evaluations are illustrated by calculating the cyclic stress ratio required to trigger liquefaction of clean sand (i.e., CRR) at a depth of 30-m with an SPT  $N_{60}$  of 50 and  $\sigma'_v/P_a = 4$  (corresponding to a 10-m deep water table and reasonable total unit weights).

#### Using Current $C_N$ and $K_\sigma$ Relations

First, the SPT  $N_{60}$  is corrected for overburden stress using the relation by [15]:

$$C_N = \left( \frac{P_a}{\sigma'_v} \right)^{0.5} = (1/4)^{0.5} = 0.50 \quad (30)$$

$$(N_1)_{60} = 0.5 \cdot 50 = 25 \quad (31)$$

The value of  $CRR_{\sigma=1, \alpha=0}$  estimated using equation (3) is:

$$CRR_{\sigma=1, \alpha=0} = \exp \left\{ \begin{aligned} & \left[ \frac{25}{14.1} + \left( \frac{25}{126} \right)^2 \right] \\ & - \left[ \left( \frac{25}{23.6} \right)^3 + \left( \frac{25}{25.4} \right)^4 \right] - 2.8 \end{aligned} \right\} \quad (32)$$

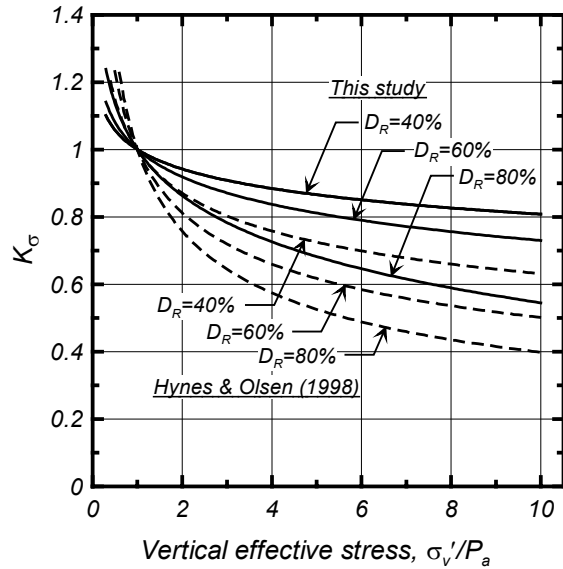


Fig. 11: Comparison of derived  $K_\sigma$  relations to those recommended by [13].

$$CRR_{\sigma=1, \alpha=0} = 0.290 \quad (33)$$

$K_\sigma$  is obtained using the relation by [16],

$$K_\sigma = \left( \frac{P_a}{\sigma'_v} \right)^{1-f} \quad (34)$$

for which the recommended values for  $f$  that were adopted in [13] were 0.8 at  $D_R=40\%$ , 0.7 at  $D_R=60\%$ , and 0.6 at  $D_R=80\%$ . These values of  $f$  are linearly related to  $D_R$  as,

$$f = 1 - \frac{D_R}{2} \quad (35)$$

which results in the following equation for application,

$$K_\sigma = \left( \frac{P_a}{\sigma'_v} \right)^{D_R/2} \quad (36)$$

The  $D_R$  and  $K_\sigma$  values for this example are then:

$$D_R = \sqrt{\frac{25}{46}} = 0.74 \quad (37)$$

$$K_\sigma = \left( \frac{1}{4} \right)^{0.74/2} = 0.60 \quad (38)$$

Finally, the CRR is obtained as:

$$CRR = 0.290 \cdot 0.60 = 0.174 \quad (39)$$

*Using  $C_N$  and  $K_\sigma$  Relations Derived Herein*

First, the proposed equations for  $C_N$  and  $(N_1)_{60}$ , which reference each other, are written in separate cells of an Excel spreadsheet and solved by turning on the

“Iterations” option as previously described. The converged solution is:

$$C_N = \left( \frac{1}{4} \right)^{0.784 - 0.0768\sqrt{(N_1)_{60}}} = 0.61 \quad (40)$$

$$(N_1)_{60} = C_N \cdot 50 = 30.3 \quad (41)$$

The  $CRR_{\sigma=1, \alpha=0}$ ,  $K_\sigma$ , and CRR values are then obtained as:

$$CRR_{\sigma=1, \alpha=0} = \exp \left\{ \frac{30.3}{14.1} + \left( \frac{30.3}{126} \right)^2 - \left( \frac{30.3}{23.6} \right)^3 + \left( \frac{30.3}{25.4} \right)^4 - 2.8 \right\} \quad (42)$$

$$CRR_{\sigma=1, \alpha=0} = 0.506 \quad (43)$$

The values of  $K_\sigma$  and CRR for this example are then equal to:

$$C_\sigma = \frac{1}{18.9 - 2.55\sqrt{30.3}} = 0.206 \quad (44)$$

$$K_\sigma = 1 - 0.206 \cdot \ln\left(\frac{4}{1}\right) = 0.71 \quad (45)$$

$$CRR = 0.506 \cdot 0.71 = 0.361 \quad (46)$$

This estimate of CRR is 107% greater than the value obtained above using relations currently utilized in practice. Of this difference, about 18% can be attributed to the difference in  $K_\sigma$  (i.e., 0.71 versus 0.60) and the remainder is due to the difference in  $C_N$  (0.61 versus 0.50) which affected the  $(N_1)_{60}$  values and hence the predicted  $CRR_{\sigma=1, \alpha=0}$  values.

*Using the  $C_\xi$  Approach*

First, the solution for  $C_N$  and  $(N_1)_{60}$  proceeds in the same manner as outlined in the previous section. Then the state normalized penetration resistance is obtained as:

$$C_\xi = \frac{\left( \sqrt{(N_1)_{60}} - \frac{6.78}{5.85 - \ln\left(\frac{\sigma'_v}{P_a}\right)} + 1.16 \right)^2}{(N_1)_{60}} = 0.87 \quad (47)$$

$$N_{1\xi} = 0.87 \cdot 30.3 = 26.5 \quad (48)$$

Finally, the CRR is obtained as:

$$CRR = \exp \left\{ \frac{26.5}{14.1} + \left( \frac{26.5}{126} \right)^2 - \left( \frac{26.5}{23.6} \right)^3 + \left( \frac{26.5}{25.4} \right)^4 - 2.8 \right\} \quad (49)$$

$$CRR = 0.330 \quad (50)$$

This CRR is about 9% smaller than the value obtained using the derived  $K_\sigma$  relations. This small difference in CRR values is due solely to the approximations involved

TABLE 1: CRR VALUES PREDICTED BY CURRENT VERSUS PROPOSED RELATIONS

$\sigma_v'/P_a$ (N) <sub>60</sub>	Using current $C_N$ and $K_\sigma$ relations					Using proposed $C_N$ and $K_\sigma$ relations					Using proposed $C_N$ and $C_\xi$ relations					
	$C_N$	(N) <sub>60</sub>	$CRR_{\sigma=1}$	$K_\sigma$	CRR	$C_N$	(N) <sub>60</sub>	$CRR_{\sigma=1}$	$K_\sigma$	CRR	$C_N$	(N) <sub>60</sub>	$C_\xi$	(N) <sub>60</sub>	CRR	
2	10	0.71	7.1	0.099	0.87	0.086	0.67	6.7	0.096	0.94	0.091	0.67	6.7	0.88	5.9	0.091
2	20	0.71	14.1	0.149	0.83	0.123	0.71	14.2	0.150	0.93	0.138	0.71	14.2	0.92	13.0	0.140
2	30	0.71	21.2	0.222	0.79	0.175	0.75	22.4	0.240	0.90	0.215	0.75	22.4	0.94	21.0	0.218
2	40	0.71	28.3	0.396	0.76	0.301	0.78	31.3	0.579	0.85	0.493	0.78	31.3	0.95	29.6	0.459
4	20	0.50	10.0	0.118	0.72	0.085	0.47	9.3	0.114	0.88	0.099	0.47	9.3	0.78	7.3	0.100
4	30	0.50	15.0	0.156	0.67	0.105	0.51	15.4	0.159	0.84	0.134	0.51	15.4	0.82	12.7	0.137
4	40	0.50	20.0	0.206	0.63	0.130	0.56	22.3	0.238	0.80	0.190	0.56	22.3	0.85	19.0	0.195
4	50	0.50	25.0	0.290	0.60	0.174	0.61	30.3	0.506	0.71	0.361	0.61	30.3	0.87	26.5	0.330
4	60	0.50	30.0	0.485	0.57	0.277	0.66	39.5	>2	0.52	>0.60	0.66	39.5	0.89	35.1	>0.60
8	30	0.35	10.6	0.122	0.61	0.074	0.32	9.7	0.116	0.81	0.094	0.32	9.7	0.63	6.1	0.093
8	50	0.35	17.7	0.180	0.52	0.095	0.40	20.0	0.206	0.72	0.149	0.40	20.0	0.73	14.7	0.154
8	70	0.35	24.7	0.284	0.47	0.133	0.51	35.6	1.249	0.44	0.545	0.51	35.5	0.80	28.3	0.396
8	90	0.35	31.8	0.626	0.42	0.264	0.58	52.1	>2	0.38	>0.60	0.58	52.1	0.82	42.7	>0.60
Equations:	(30)	(5)	(3)	(8, 36)	(1)	(10)	(5)	(3)	(26,28)	(1)	(10)	(5)	(17)	(12)	(21)	

in deriving the  $K_\sigma$  relations from the  $\xi_R$ -framework results.

*Comparisons of Approaches for Other Conditions*

Table 1 contains comparisons of the three approaches for a range of  $N_{60}$  values and  $\sigma_v'/P_a$  of 2, 4 and 8. The two approaches proposed herein (either the  $C_\xi$  approach, or the corresponding  $K_\sigma$  relations) give quite similar results as expected. Both of these approaches give significantly greater CRR values than those obtained using the common  $C_N$  by [15] and  $K_\sigma$  recommended by [13]. The difference is relatively small for loose sands, but becomes increasingly significant as  $D_R$  increases and the overburden stress increases. As illustrated in the examples, the differences are due to the changes in both  $C_N$  and  $K_\sigma$  (or alternatively  $C_\xi$ ).

CONCLUSIONS

Recent developments have provided a consistent theoretical framework for inter-relating the  $C_N$  and  $K_\sigma$  factors, both of which are important for evaluating liquefaction resistance of sand at high overburden stresses [2][3][4][5]. State normalization of penetration resistances was shown to be a technically attractive alternative to the use of the traditional  $K_\sigma$  factors. This paper built upon these theoretical developments by deriving new equations that are easily implemented in practice and demonstrating their application and impact through an example. It is hoped that the suggested approach will provide a useful means for augmenting the current field-based methods for evaluating liquefaction potential in engineering practice.

REFERENCES

[1] H. B. Seed, "Earthquake resistant design of earth dams." Proc., Symposium on Seismic Design of Embankments and Caverns, Pennsylvania, ASCE, N.Y., 1983, pp. 41-64.

[2] R. W. Boulanger, "Relating  $K_a$  to relative state parameter index." J. Geotechnical and Geoenvironmental Engineering, ASCE, 2003, 129(8), 770-773.

[3] R. W. Boulanger, "High overburden stress effects in liquefaction evaluations." J. Geot. & Geoenv. Eng, ASCE, 2003, 129(12), 1071-1082.

[4] I. M. Idriss and R. W. Boulanger, "'Estimating  $K_a$  for use in evaluating cyclic resistance of sloping ground." Proc. 8th US-Japan Workshop on Earthquake Resistant Design of Lifeline Facilities and Countermeasures against Liquefaction, Hamada, O'Rourke, and Bardet, eds., Report MCEER-03-0003, MCEER, SUNY Buffalo, N.Y., 2003, 449-468.

[5] I. M. Idriss and R. W. Boulanger, "Relating  $K_a$  and  $K_\sigma$  to SPT Blow Count and to CPT Tip Resistance for Use in Evaluating Liquefaction Potential." Proceedings of the 2003 Dam Safety Conference, ASDSO, September 7 – 10, 2003, Minneapolis.

[6] M. D. Bolton, "The strength and dilatancy of sands." Geotechnique, 1986, 36(1), 65-78.

[7] Y. P. Vaid and S. Sivathayalan, "Static and cyclic liquefaction potential of Fraser Delta sand in simple shear and triaxial tests." Canadian Geotechnical Journal, 1996, 33, 281-289.

[8] Y. P. Vaid, and J. Thomas, "Liquefaction and postliquefaction behavior of sand." J. Geotech. Engrg., ASCE, 1995, 121(2), 163-173.

[9] H. B. Seed, "Soil liquefaction and cyclic mobility evaluation for level ground during earthquakes." J. Geotechnical Engineering Division, ASCE, 1979, 105(GT2), 201-255.

[10] I. M. Idriss, "SPT-Based methods for evaluating liquefaction potential." Work in progress, 2003.

[11] I. M. Idriss, and R. W. Boulanger, "Semi-empirical procedures for evaluating liquefaction potential during earthquakes." Proc., 11<sup>th</sup> Int. Conf. Soil Dynamics and Earthquake Engrg., and 3<sup>rd</sup> Int. Conf. Earthquake Geotechnical Engrg., University of California, Berkeley, CA, January, 2004.

[12] L. F. Harder, Jr., and R. W. Boulanger, "Application of  $K_\sigma$  and  $K_a$  correction factors." Proc., NCEER Workshop on Evaluation of Liquefaction Resistance of Soils, Report NCEER-97-0022, MCEER, SUNY Buffalo, N.Y., 1997, pp. 167-190.

[13] T. L. Youd et al., "Liquefaction resistance of soils: Summary report from the 1996 NCEER and 1998 NCEER/NSF workshops on evaluation of liquefaction resistance of soils." J. Geotech. and Geoenvir. Engrg., ASCE, 2001, 127(10), 817-833.

[14] H. B. Seed, K. Tokimatsu, L. F. Harder, Jr., and R. Chung, "Influence of SPT procedures in soil liquefaction resistance evaluations." J. Geotechnical Engineering, ASCE, 1985, 111(12), 1425-1445.

[15] S. C. Liao and Whitman, R. V., "Overburden correction factors for SPT in sand." J. Geot. Engrg., ASCE, 1986, 112(3), 373-377.

[16] M. E. Hynes and R. Olsen, "Influence of confining stress on liquefaction resistance." Proc., Intl. Symp. on the Physics and Mechanics of Liquefaction, Balkema, 1998, 145-152.